A Unified Approach to Surface-Enhanced Raman Spectroscopy

John R. Lombardi* and Ronald L. Birke

Department of Chemistry, The City College of New York, New York, New York 10031

Received: January 8, 2008

We present a unified expression for surface-enhanced Raman spectroscopy (SERS). The expression contains a product of three resonance denominators, representing the surface plasmon resonance, the metal−molecule charge-transfer resonance at the Fermi energy, and an allowed molecular resonance. This latter resonance is that from which intensity is borrowed for charge transfer, and when the molecular resonance is active it is responsible for surface-enhanced resonance Raman spectroscopy. We examine this expression in various limits, to explore the relative contribution or each resonance. First, we look at the situation in which only the surface plasmon resonance is active and examine the various contributions to the Raman signal, including the surface selection rules. Then we examine additional contributions from charge-transfer or molecular resonances. We show that the three resonances are not totally independent, since they are linked by a product of four matrix elements in the numerator. These linked matrix elements provide comprehensive selection rules for SERS. One involves a harmonic oscillator in the observed normal mode. This is the same mode which appears in the vibronic coupling operator linking one of the states of the allowed molecular resonance to the charge-transfer state. The charge-transfer transition moment is linked to the surface plasmon resonance by the requirement that the transition dipole moment be polarized along the direction of maximum amplitude of the field produced by the plasmon (i.e., perpendicular to the metal surface). We show that these selection rules govern the observed SERS spectral intensities and apply these to the observed spectra of several molecules. We also suggest a quantitative measure of the degree to which charge transfer contributes to the overall SERS enhancement.

I. Introduction

The discovery of very large enhancements of the Raman signal[1−4] induced by proximity to a metal surface has led to numerous interesting and valuable developments in nanoscience. The effect is of sufficient interest that a rather large number of investigations have been carried out using a variety of substrates and examining many different molecular species. The consequence of all this interest is that the numerous manifestations of the effect are difficult to explain using a simple theory. It was first realized that the nature of the conduction band of the metal and the need for nanoscale surface features implies that a surface plasmon resonance must be important for the effect to be observed. However, examination of the potential dependence of the effect in electrochemical[5−7] experiments led several investigators[8−10] to propose that a charge-transfer resonance between the molecule and the metal was also of importance. More recently, even larger enhancements have been discovered, by examining systems on the single molecule level.[11−13] These were observed with single molecules adsorbed on one or between two or more Ag nanoparticles.[14−17] Although the rather large enhancements observed have been cited as possible evidence for charge-transfer contributions, other, more recent work presents a reinterpretation of the magnitude of the enhancement in these experiments.[18] Most of these single molecule experiments were carried out choosing molecules, which in addition to the surface plasmon and charge-transfer resonances, have a molecular resonance in the range of excitation. These considerations lead to the conclusion that it is important to consider the molecule and metal as a single system. The states involved in various resonances should be regarded as part of this molecule−metal system, and all properties are affected by this interaction. The plasmon resonance is mostly a property of the metal, while the molecular resonances are properties mostly of the molecule. The charge-transfer states are properties of the combined system. Thus, in order to fully explain the observations, three types of resonance may need to be invoked. However, at any single excitation frequency, it is often difficult to distinguish the degree to which each of the type of resonance contributes to the overall enhancement. In order to obtain a complete picture of the relative contribution of each resonance, experiments must be carried out at a wide variety of excitation wavelengths,[19] by electrochemically varying the applied potential or possibly by varying the location of the surface plasmon resonance by carefully controlling particle size[20] or interparticle distance.[21] We will show that we if we are in the region of a charge-transfer or molecular resonance, the enhancement of the nontotally symmetric bands relative to the totally symmetric bands will vary. In the absence of charge-transfer contributions, the relative enhancement of both types of bands should be the same.

In this Article, we present a single expression for the enhancement, which includes all three types of resonance in the denominator, while all three effects are linked by a product of four matrix elements in the numerator. This means that surface-enhanced Raman spectroscopy (SERS) need not be explained as a coincidence of several disparate effects, but can be considered a single effect drawing on up to three resonances which are intimately tied to each other and cannot easily be considered separately. Depending on the parameters associated with each resonance at each excitation wavelength as well as the selection rules, the various resonances contribute differing

10.1021/jp800167v CCC: $40.75
Published on Web 03/19/2008

amounts to the enhancement, and it is our intention in this Article to clarify the ways in which each contribution may be extracted. In the next section, we examine the resonances separately, starting with the surface plasmon resonance. We show that even far from charge-transfer or molecular resonance, these transitions can influence the observed spectrum. We examine the differences between SERS and normal Raman spectroscopy, to identify the special contributions made to the Raman spectrum by proximity to the metal surface. Especially important is the preferential polarization of light normal to the surface, and this leads to an examination of the sources of the surface selection rules. We then examine the additional contributions due to an overlap of the surface plasmon resonance with either a charge-transfer or molecular resonance (or both). This imposes further symmetry requirements on the spectrum and leads us to examine the resulting Herzberg−Teller-surface selection rules. As a stringent test of these selection rules, we apply them to the observed SERS spectra of a series of rather symmetric molecules, including the azines, benzene, and the less symmetric berberine. Some of these comparisons are necessarily qualitative, due to lack of sufficient data, so that we then examine more quantitatively the spectrum of a molecule (*p*-aminothiophenol) for which considerable data has been obtained. We define an experimental parameter (the degree of charge transfer), which enables us to examine the various contributions to the SERS intensity for a wide variety of excitation wavelengths and substrates.

II. Surface-Enhanced Raman Spectroscopy (SERS)

The intensity of a Raman transition may be obtained from the polarizability tensor by the expression

$$I = [8\pi(\omega \pm \omega_{I'I})^4 I_L/9c^4] \sum \alpha_{\sigma\rho}{}^2 \quad (1)$$

where I_L is the incident laser intensity at ω and $\omega_{I'I}$ is a molecular transition frequency between states I and I′ (presumably two different vibronic levels of the ground electronic state I_e). The subscripts σ and ρ represent the three directions in space (X, Y, Z) and together make up the nine components of the polarizability tensor.

A. The Surface Plasmon Resonance. When the dielectric constant of a metal has a negative real component, combined with a small imaginary component, the metal is capable of sustaining a surface plasmon resonance (SPR). This resonance represents a coherent oscillation of the surface conduction electrons when excited by electromagnetic radiation. The excited state of the plasmon can be described as a correlated many-electron excitation of all possible electron−hole pairs, for which the energy separation matches the laser frequency.[15] In bulk silver this resonance is in the near-ultraviolet region of the spectrum. For a metal nanoparticle, the plasmon resonance is localized near the surface of the particle, and it is found that considerably larger enhancements may be obtained by aggregates of two or more nanoparticles oscillating collectively. Furthermore, the enhanced electric field at the particle surface is strongly influenced by the details of the shape of the nanoparticle, and many creative techniques to control the shape and size of an array of such particles have recently been developed.[20] For example, triangular silver nanoparticles display several dipolar as well as quadrupolar resonances farther to the red of the dipolar resonance observed in a spherical particle.[22] The combination of collective oscillations of nanoparticle arrays as well as various selected shapes has extended the range of useful localized surface plasmon effects throughout the visible and near-infrared region of the spectrum. Equation 1 implies that a vibrating molecule located near a metal nanoparticle array will couple to the exciting light; i.e., the polarizability tensor of the metal−molecule system couples to the SPR field.

The plasmon resonance[23−25] may be discussed by examining the term I_L. For Raman spectroscopy, it can be shown to be proportional to the electromagnetic enhancement factor $L^2(\omega_L)L^2(\omega_S)$ where ω_L and ω_S are the incident and scattered Raman frequencies, respectively, and $L(\omega) = E_R/E_0$ where E_R is SPR field and E_0 is the incident field of the exciting light. This gives an electromagnetic enhancement factor of $[E_R/E_0]^4$, but it should be appreciated that such a relationship is not strictly valid for hot-spot scattering due to a collection of metal particles.[26] However, for simplicity, we first examine the simple model of a single sphere embedded in an environment of dielectric constant ϵ_0; this factor may be related to the radius of the spherical metal particle a, the distance of the molecule from the center of the metal particle r, and g a function of the complex dielectric function $\epsilon(\omega_L) = \epsilon_1 + i\epsilon_2$ as follows:

$$L^2(\omega_L)L^2(\omega_S) \approx |g(\omega_L)|^2|g(\omega_S)|^2 \approx |(g\,(a/r)^3|^4) \quad (2)$$

$$g(\epsilon) = [\epsilon(\omega) - \epsilon_0]/[\epsilon(\omega) + 2\epsilon_0] = [\epsilon(\omega) - \epsilon_0]/[\epsilon_1(\omega) + 2\epsilon_0 + i\epsilon_2(\omega)] \quad (3)$$

Letting $\omega_L \approx \omega_S = \omega$, it can be seen that for frequencies at which $\epsilon_1 = -2\epsilon_0$ resonance is obtained and that the enhancement factor is proportional to $\epsilon_2{}^{-4}$. For silver in the near-ultraviolet region, the resonance condition holds ($\epsilon_0 = 1.77$ for water, $\epsilon_1 = -3.54$ and $\epsilon_2 = 0.11$ at 382 nm for bulk Ag), while in this same region ϵ_2 is small. This is the source of the surface plasmon resonance, and it is presumed to produce a very large electric field normal to the metal surface. It should be pointed out that typically ω_L is only approximately equal to ω_S, so the approximation in eq 2 may not hold in certain spectral ranges especially if a molecule is at a location between two metal particles.[27] For situations in which the difference between ω_L and ω_S is larger than the resonance widths, it is found that the optimum enhancement is obtained approximately halfway between. Since we are interested in examining spectral intensities of both totally and nontotally symmetric normal modes, we are also interested in the relative strength of the normal and tangential component of the electric vector of both the incoming and outgoing light. For a sphere of radius a, the normal (n) and tangential (t) components are given by

$$L_n(\omega) = (^1/_3)^{1/2}E_0[1 + 2g(\epsilon)(a/r)^3]$$
$$L_t(\omega) = (^2/_3)^{1/2}E_0[1 - g(\epsilon)(a/r)^3] \quad (4)$$

Note that at resonance ($g(\epsilon) \gg 1$) for a sphere, the tangential-to-normal fields are almost equal. For a prolate spheroid, the expressions are somewhat more complex,[28] and they are functions of the prolate spheroidal coordinates (ξ, η, φ). Then the normal and tangential components may be written as

$$L_n{}^2(\omega) = \eta^2\left(\frac{\xi^2 - 1}{\xi^2 - \eta^2}\right)w \quad L_t{}^2(\omega) = \xi_0{}^2\left(\frac{1 - \eta^2}{\xi_0{}^2 - \eta^2}\right)w \quad (5)$$

where w is a factor involving Legendre functions and ξ_0 is the value of ξ at the particle surface. It is found that near the particle tip ($\eta = \pm 1$) the enhancement is the largest. At that point the tangential field is zero. On the other hand, at other points along the ellipsoidal surface the ratio of the tangential/normal field increases. At the equator of the ellipsoid, the field is entirely

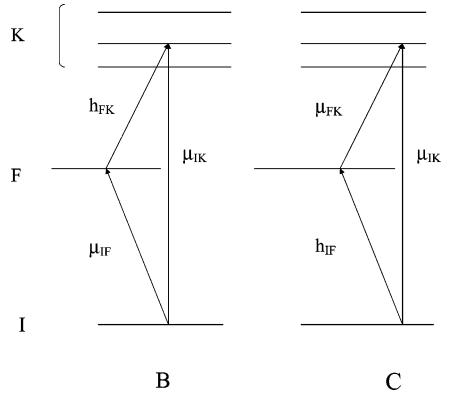

Figure 1. State diagram of molecule−metal system. Transitions are allowed from the molecular ground state $|I\rangle$ to one or more of the excited states $|K\rangle$ through μ_{IK}. For the B term, a molecule → metal charge-transfer transition to the Fermi state $|F\rangle$ is allowed through μ_{IF}. The states $|F\rangle$ and $|K\rangle$ are connected through the Herzberg−Teller vibronic coupling term h_{KF}. For the C term, a metal → molecule charge-transfer transition from the Fermi state $|F\rangle$ is allowed through μ_{KF}. The states $|F\rangle$ and $|I\rangle$ are connected through the Herzberg−Teller vibronic coupling term h_{IF}.

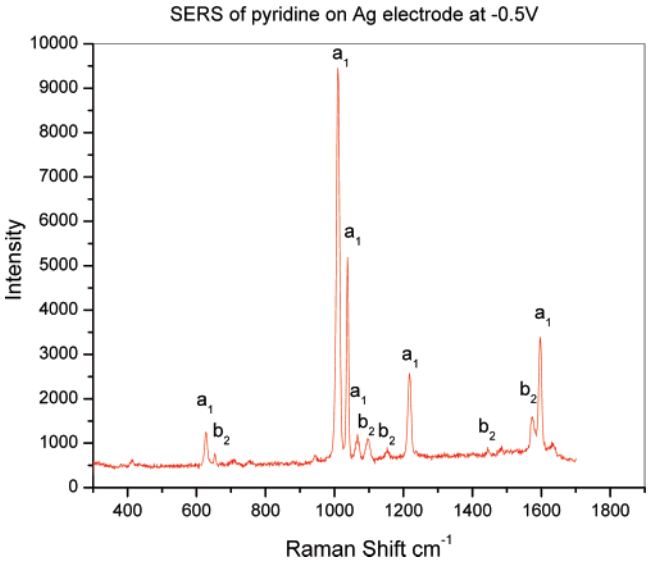

Figure 2. Surface-enhanced Raman spectrum of pyridine on Ag electrode. The symmetry species of the most enhanced modes (a_1 and b_2) are shown. All other modes are much weaker or not seen.

tangential ($\eta = 0$). This is important because it illustrates the fact that for certain nanoparticle geometries, we might expect that the largest enhancements are near points or hot spots on the surface, and in that region the normal component of the field is much larger than the tangential component. Where two or more nanoparticles are near each other, we expect the hot spots to be near the juncture of the two particles. Gersten and Niztan[29] show theoretically for a simple model of a two-spheres cluster that the electromagnetic (EM) flux is concentrated in the region between the spheres, and more recently this type of EM enhancement has been investigated experimentally and theoretically.[15,30,31] For a molecule located between two such particles, the points at which the molecule would be inserted[31] can be considered tips, and once again tip effects are likely to be important. Even if the geometry is not the same as an ellipsoid, but instead, say, a pyramid or other structure, the field directions and relative intensities should be similar to those near the ellipsoidal tip.

We now consider the situation in which the surface plasmon is in or near resonance with the laser, and we are far from

TABLE 1: Low-Lying Singlet Electronic States of Pyridine[a]

state	type	T_{00} (cm^{-1})	T_{00} (eV)	intensity
$^1A_1$	X	0	0	
$^1B_1$	n → π^*	34 770	4.31	$f = 0.003$
$^1B_2$	$\pi \rightarrow \pi^*$	33 850	4.75	$f = 0.04$
$^1A_1$	$\pi \rightarrow \pi^*$	49 750	6.17	$f = 0.10$
$^1B_2$	$\pi \rightarrow \pi^*$	55 000	6.82	$f = 1.3$
$^1A_1$	$\pi \rightarrow \pi^*$	56 405	6.99	

[a] See ref 49.

charge-transfer or molecular resonances. The general expression for the polarizability tensor for the molecule−metal system may be written as

$$\alpha_{\sigma\rho} = \sum_{S \neq I,I'} \left\{ \frac{\langle I|\mu_\sigma|S\rangle\langle S|\mu_\rho|I'\rangle}{E_S - E_I - \hbar\omega} + \frac{\langle I|\mu_\rho|S\rangle\langle S|\mu_\sigma|I'\rangle}{E_S - E_I + \hbar\omega} \right\} \quad (6)$$

where S represents all the excited states of the system, μ is the dipole moment operator, and σ,ρ are the scattered and incident polarization directions. This is the standard Kramers, Heisenberg, and Dirac (KHD)[32,33] expression, and using the zero-order Born−Oppenheimer approximation, we may write all the vibronic states (I, I′, S) as products of the electronic and vibrational wave functions: $|I\rangle = |I_e\rangle|i\rangle$, $|I'\rangle = |I_e\rangle|f\rangle$, and $|S\rangle = |S_e\rangle|k\rangle$, where the subscript e indicates a purely electronic state and lower-case letters represent vibrational functions. Albrecht[34] utilized the Herzberg−Teller mixing of vibronic functions

$$|S\rangle = |S_e,0\rangle + \sum \lambda_{SR} Q |R_e,0\rangle \quad (7)$$

$$\lambda_{SR} = h_{SR}/(E_R^0 - E_S^0) \quad (8)$$

$$h_{SR} = \langle S_e,0|(\partial V_{eN}/\partial Q)_0|R_e,0\rangle \quad (9)$$

to derive an expression for $\alpha_{\sigma\rho}$ which involves the sum of three terms, usually called A, B, and C. V_{eN} is the electron−nuclear attraction term in the Hamiltonian, evaluated at the equilibrium nuclear positions (0). For the purely electronic transition moment between states, we write $\mu^\sigma_{SI} = \langle S_e|\mu^\sigma|I_e\rangle$, $\mu^\sigma_{RI} = \langle R_e|\mu^\sigma|I_e\rangle$, and $\mu^\sigma_{SR} = \langle S_e|\mu^\sigma|R_e\rangle$.

In previous work (I[35] and II[36]), we applied these ideas to SERS . We assumed that the molecule was bound to the metal surface through a weak covalent bond and that the molecule−metal system may be considered together for purposes of calculations. Thus, the metal conduction band (M) must be included in the A, B, and C terms derived by Albrecht. In earlier work, Albrecht showed that intensity borrowing from the same allowed transitions was also responsible for appearance of forbidden character in optical spectra.[37,38] When the molecule is not coupled to the metal, charge-transfer transitions between the molecule and metal are forbidden. On coupling, charge-transfer intensity is borrowed from some allowed molecular transition μ_{KI} by the molecule-to-metal transition μ_{IM} through the Herzberg−Teller coupling term h_{MK} or by the metal-to-molecule transition μ_{MK} through the Herzberg−Teller coupling term h_{IM}. Focusing primarily on the charge-transfer contributions, we have previously shown (I and II) that SERS charge-transfer intensity is maximized when the metal state involved is at the Fermi energy. The practical result is that in the equations we may remove the sum over M states and replace M with the appropriate charge-transfer state F (See Figure 1). Note that the Fermi energy varies with applied potential, so that in electrochemical experiments, we obtain an expression for the potential

dependence observed in SERS (see section B below). We then obtain analogues of the Albrecht A, B, and C terms for the molecule−metal system.

$$\alpha_{\sigma\rho} = \mathrm{A} + \mathrm{B} + \mathrm{C} \tag{10}$$

$$\mathrm{A} = \sum_{\mathrm{S=F,K}\neq\mathrm{I}} \sum_{k} \left[\frac{\mu^{\sigma}_{\mathrm{SI}}\mu^{\rho}_{\mathrm{SI}}}{\hbar(\omega_{\mathrm{SI}} - \omega)} + \frac{\mu^{\rho}_{\mathrm{SI}}\mu^{\sigma}_{\mathrm{SI}}}{\hbar(\omega_{\mathrm{SI}} + \omega)} \right] \langle \mathrm{i}|\mathrm{k}\rangle\langle \mathrm{k}|\mathrm{f}\rangle$$

$$\mathrm{B} = \sum_{\mathrm{R=F,K}} \sum_{\mathrm{S=F,K}} \sum_{k} \left[\frac{\mu^{\sigma}_{\mathrm{IR}} h_{\mathrm{RS}} \mu^{\rho}_{\mathrm{SI}}}{\hbar(\omega_{\mathrm{RI}} - \omega)} + \frac{\mu^{\rho}_{\mathrm{IR}} h_{\mathrm{RS}} \mu^{\sigma}_{\mathrm{SI}}}{\hbar(\omega_{\mathrm{RI}} + \omega)} \right] \frac{\langle \mathrm{i}|\mathrm{k}\rangle\langle \mathrm{k}|\mathrm{Q}_k|\mathrm{f}\rangle}{\hbar\omega_{\mathrm{RS}}} +$$

$$\sum_{\mathrm{R=F,K}} \sum_{\mathrm{S=F,K}} \sum_{k} \left[\frac{\mu^{\sigma}_{\mathrm{IS}} h_{\mathrm{SR}} \mu^{\rho}_{\mathrm{RI}}}{\hbar(\omega_{\mathrm{RI}} - \omega)} + \frac{\mu^{\rho}_{\mathrm{IS}} h_{\mathrm{SR}} \mu^{\sigma}_{\mathrm{RI}}}{\hbar(\omega_{\mathrm{RI}} + \omega)} \right] \frac{\langle \mathrm{i}|\mathrm{Q}_k|\mathrm{k}\rangle\langle \mathrm{k}|\mathrm{f}\rangle}{\hbar\omega_{\mathrm{RS}}}$$

$$\mathrm{C} = \sum_{\mathrm{R=F,K}} \sum_{\mathrm{S=F,K}} \sum_{k} \left[\frac{\mu^{\sigma}_{\mathrm{IR}} h_{\mathrm{IS}} \mu^{\rho}_{\mathrm{SR}}}{\hbar(\omega_{\mathrm{RI}} - \omega)} + \frac{\mu^{\rho}_{\mathrm{IR}} h_{\mathrm{IS}} \mu^{\sigma}_{\mathrm{SR}}}{\hbar(\omega_{\mathrm{RI}} + \omega)} \right] \frac{\langle \mathrm{i}|\mathrm{k}\rangle\langle \mathrm{k}|\mathrm{Q}_k|\mathrm{f}\rangle}{\hbar\omega_{\mathrm{SI}}} +$$

$$\sum_{\mathrm{R=F,K}} \sum_{\mathrm{S=F,K}} \sum_{k} \left[\frac{\mu^{\sigma}_{\mathrm{SR}} h_{\mathrm{IS}} \mu^{\rho}_{\mathrm{IR}}}{\hbar(\omega_{\mathrm{RI}} - \omega)} + \frac{\mu^{\rho}_{\mathrm{SR}} h_{\mathrm{IS}} \mu^{\sigma}_{\mathrm{IR}}}{\hbar(\omega_{\mathrm{RI}} + \omega)} \right] \frac{\langle \mathrm{i}|\mathrm{Q}_k|\mathrm{k}\rangle\langle \mathrm{k}|\mathrm{f}\rangle}{\hbar\omega_{\mathrm{SI}}}$$

When, as presumed in this section, we are far from any charge-transfer or molecular resonance, the denominators in the above expressions are all approximately the same and may be removed from the sums. In the A term, we then make use of the closure relation $\Sigma|\mathrm{k}\rangle\langle\mathrm{k}| = 1$ and the orthogonality expression $\langle \mathrm{i}|\mathrm{f}\rangle = \delta_{\mathrm{if}}$. Thus, away from resonance, the A term vanishes, and the B and C terms are entirely responsible for the surface-enhanced Raman intensity.

We should emphasize that in these expressions the sums range over all excited states (R and S) which include both charge-transfer states (F) and molecular states (K) {but of course exclude terms for which a denominator vanishes (such as S or R = I)}. This constitutes one of the important differences between SERS and normal Raman spectroscopy. The normal Raman expression[34] does not include these charge-transfer states (F). Furthermore, within these sums, these charge-transfer terms cannot be considered to be negligible. For example, in pyridine on Ag, the charge-transfer state[39] is located at about 600 nm (2.06 eV), while the lowest allowed molecular transition is at 261 nm (4.75 eV). The oscillator strengths for both transitions are comparable. For excitation at 514.5 nm (2.45 nm), it can be seen that the resonance denominator for the charge-transfer term in the sum will be much smaller (by a factor of 5) than for the next leading term. Thus, the leading term in the sum arises from a low-lying charge-transfer transition, and is about 5 times larger than the leading term in the normal Raman expression, which arises from an allowed molecular transition. It is likely that the charge-transfer transitions in many molecule−metal systems will be similarly low-lying and therefore important contributors to the SERS intensity, even when only the metal surface plasmon is in resonance.

Note also that in normal Raman spectroscopy, the molecules are usually (at least in the gas or liquid phase) randomly oriented with respect to the direction of the optical field, and to obtain a correct expression for normal Raman spectroscopy we must average over all orientations. However, for SERS, the molecule is usually adsorbed on the surface through a weak chemical bond in a definite orientation. As shown above, when the molecule is located near a special part of the nanoparticle, such as the tip of an ellipsoid or similar structure, the largest enhancements are observed. It is in just such a case that the component of the electric field normal to the surface is most intense, while the tangential component is relatively weak. This leads to the surface selection rules,[40−43] which govern the relative SERS intensities in cases where the exciting light is far from either a charge-transfer or molecular resonance.

It is convenient to consider a definite molecule when discussing these results, and we choose pyridine. In Figure 2, we present the pyridine (C_{2v}) SERS spectrum. Assuming the molecule is attached to the surface through a Ag−N bond, the C_2 axis is normal to the surface. If the most intense fields are also normal to the surface, they will pick out only certain terms in the B or C sums in the expression of eq 10. Note that terms with both σ and $\rho = Z$ (the normal direction to the surface) will be most intense. These are both of A_1 symmetry in C_{2v}. The consequence is that the Herzberg−Teller factor must also be of A_1 symmetry, and intensity borrowing takes place from an allowed $^1A_1 \rightarrow {}^1A_1$ transition. In Table 1, we give the visible and UV transitions in pyridine. It can be seen that there is such a transition at 6.17 eV (49 750 cm^{-1}) with a rather large oscillator strength. If the charge-transfer transition at 2.06 eV is of A_1 symmetry, it is easy to see that vibrations of a_1 symmetry should dominate the SERS spectrum. This is as seen in Figure 1 and is a well-known feature of many SERS spectra. We must, however, take into account the possibility that there is a nonzero tangential (*X*, *Y*) component of the electric field, because either the molecule is not located exactly at the tip of an ellipsoid (or similar structure) or possible other defects are in the idealized model. Now, terms are selected with only one component (σ or ρ) assumed to be *Z*-polarized and the other *X*- or *Y*-polarized. In this case, nontotally symmetric transitions can contribute intensity to the Raman spectrum. Since the tangential field (*X*, *Y*) is much weaker than the normal field (*Z*), we expect that these contributions will be considerably less intense than the *ZZ*-polarized terms. Also, since each term involves the square of the products of transition moments $(\mu_{\mathrm{IR}}\mu_{\mathrm{SR}})^2$, the relative SERS intensity should be proportional to the product of the respective oscillator strengths ($f_{\mathrm{IR}}f_{\mathrm{SR}}$). Note that in Table 1 there is a very weak $^1B_1$ ($n \rightarrow \pi^*$) state at 4.31 eV ($f = 0.003$) and a much stronger $^1B_2$ ($\pi \rightarrow \pi^*$) transition at 4.75 eV ($f = 0.04$). We therefore expect relatively weak vibrational bands of b_2 (*ZY*-polarized) symmetry and still weaker bands of b_1 (*ZX*-polarized) symmetry. This is exactly as observed in the spectrum. Note that any bands polarized entirely out-of-plane (i.e., both σ and ρ are either *X* or *Y*), in this case those of a_2 (*XY*-polarized) symmetry, will be extremely weak.

Careful examination of the B or C terms, therefore, will allow prediction of the SERS intensities for any molecule where only surface plasmon resonances are active. With knowledge of the relative intensity of the normal and tangential fields, we may infer the surface selection rules. The above considerations can easily be generalized to molecules with different symmetry and with different orientations with respect to the surface. If these are known, then we must also possess a good UV−vis absorption spectrum of the molecule−metal system, from which can be obtained the locations of the various molecular and charge-transfer resonances and their oscillator strengths. We may then compare leading terms in the sums to obtain relative intensities. Of course, since the total SERS intensity is the square of the sum, the possibility of interference from cross-product terms must be taken into account. The only additional term needed is the Herzberg−Teller coupling constant (eq 9) for each normal mode. This is a difficult factor to measure experimentally

(II), and it is likely that high-quality calculations will be needed to determine it. This will be discussed in more detail below.

B. Charge-Transfer and Molecular Resonances. In order to examine the situation in which the light is not only resonant with the surface plasmon but also a charge-transfer transition in the molecule−metal system, we select for examination only terms in the general expression (eq 10) above which include a charge-transfer state F. This was carried out in detail in I and II. There are two A terms, A_f and A_k. A_f and B correspond to molecule-to-metal transitions, while A_k and C correspond to metal-to-molecule transitions. In Figure 1, we illustrate the states connected by the transition moments and coupling term for both B and C.

$$A_f = (2/\hbar)\mu^{\sigma}_{FI}\mu^{\rho}_{FI}\langle i|k\rangle\langle k|f\rangle \frac{\omega_{FI} + \omega_f}{(\omega_{FI} + \omega_f)^2 - \omega^2} \quad (11)$$

$$B = -(2/\hbar^2)\sum_{K\neq I} \frac{[\mu^{\sigma}_{KI}\mu^{\rho}_{FI} + \mu^{\rho}_{KI}\mu^{\sigma}_{FI}](\omega_{KI}\omega_{FI} + \omega^2)h_{KF}\langle i|Q|f\rangle}{(\omega_{KI}{}^2 - \omega^2)(\omega_{FI}{}^2 - \omega^2)} \quad (12)$$

$$A_k = (2/\hbar)\mu^{\sigma}_{FK}\mu^{\rho}_{FK}\langle i|k\rangle\langle k|f\rangle \frac{\omega_{FK} + \omega_f}{(\omega_{FK} + \omega_f)^2 - \omega^2} \quad (13)$$

$$C = -(2/\hbar^2)\sum_{K\neq I} \frac{[\mu^{\sigma}_{KI}\mu^{\rho}_{FK} + \mu^{\rho}_{KI}\mu^{\sigma}_{FK}](\omega_{KI}\omega_{FK} + \omega^2)h_{IF}\langle i|Q|f\rangle}{(\omega^2_{KI} - \omega^2)(\omega^2_{FK} - \omega^2)} \quad (14)$$

The terms A_f and A_k are normally associated only with resonance Raman spectroscopy, since only when the denominator strikes a resonance is any appreciable intensity predicted. Far from resonance the numerator vanishes, while on resonance, the numerator restricts the observable modes to those that are totally symmetric. Furthermore, there is no restriction on overtones in these expressions, which should commonly be observed, especially if there is a large displacement in the excited-state potential minimum. However, in addition to totally symmetric modes, nontotally symmetric modes are also prominent in many SERS spectra. Thus, we must also include the B and C terms, which predict both totally and nontotally symmetric vibrations to be active. To the extent that the A term contributes to the totally symmetric modes of SERS, it is *in addition* to the totally symmetric contributions to those modes from the B or C term.

In the following discussion, for simplicity we restrict ourselves to metal-to-molecule charge transfer (C). The corresponding expressions for molecule-to-metal transfer may be obtained simply by interchanging I and K. Combining eqs 1, 3, and 14 and eliminating (for clarity) extraneous factors and sums, we obtain the following expression:

$$R_{IFK}(\omega) = \frac{\mu_{KI}\mu_{FK}h_{IF}\langle i|Q_k|f\rangle}{((\epsilon_1(\omega) + 2\epsilon_0)^2 + \epsilon_2^2)((\omega^2_{FK} - \omega^2) + \gamma^2_{FK})((\omega^2_{IK} - \omega^2) + \gamma^2_{IK})} \quad (15)$$

The SERS charge-transfer enhancement factor is proportional to $|R_{IFK}(\omega)|^2$. Let us first examine the denominator, which involves the product of three terms, each of which depicts a different resonance contribution to SERS. The first $((\epsilon_1(\omega) + 2\epsilon_0)^2 + \epsilon_2{}^2)$ is due to the plasmon resonance at $\epsilon_1(\omega) = -2\epsilon_0$. We choose this expression for a single particle for illustrative purposes, recognizing that for particle aggregates with hot spots a more complex expression containing the same dielectric resonance expression will be required.[31] The second resonance, which may be potential (Fermi energy)-dependent and represents charge-transfer resonance $(\omega^2_{FK} - \omega^2) + \gamma^2_{FK}$ occurs at $\omega = \omega_{FK}$, and the third $(\omega^2_{IK} - \omega^2) + \gamma^2_{IK}$ represents the molecular resonance at $\omega = \omega_{IK}$. For electrochemical SERS, the expression for the second resonance in the C term predicts a positive slope for V_{MAX} (the applied voltage at resonance) against ω for metal-to-molecule transfer, and the B term predicts the opposite (negative) slope for molecule-to-metal transfer ($\omega = \omega_{FI,K} = E_F(0) \pm eV_{MAX}$).[7] Note that in the third case, if the resonance condition is fulfilled ($\omega = \omega_{IK}$) we have surface-enhanced resonance Raman spectroscopy (SERRS). This is the case for most of the single molecule experiments, such as rhodamine 6G, for which the molecular transition is also in resonance with the laser. Thus, the denominator of eq 15 predicts the possibility of one, two, or three resonances simultaneously, depending on the metallic and molecular parameters. If each resonance equally contributed a factor of 10^3-10^4, which is possible (depending on the values of the damping parameters ϵ_2, γ_{FK}, and γ_{IK}), we can predict enhancements of 10^3-10^4 for one resonance, 10^6-10^8 for two resonances, and 10^9-10^{12} for the coincidence of all three resonances. Of course, all three damping parameters (not to mention resonance conditions) are not usually equal, so that each term will contribute to a different degree in an actual experiment at any given excitation wavelength. It should also be pointed out that for any of the resonances the enhancement factor is proportional to the inverse fourth power of the corresponding damping parameter γ^{-4} (where γ is ϵ_2, γ_{FK}, or γ_{IK}). Thus, the magnitude of the SERS enhancement is extremely sensitive to the magnitude of these parameters.

In order to obtain a complete picture of the relative contribution of each resonance, experiments must be carried out either at a wide variety of excitation wavelengths, by electrochemically varying the applied potential or possibly by varying the location of the surface plasmon resonance by carefully controlling particle size or interparticle distance.

We now examine the numerator in eq 15, which provides the selection rules for SERS. It is important to observe that all four terms in the numerator are linked to each other. First note that the Herzberg−Teller effect contributes a product of $h_{IF} = \langle I|\partial V_{eN}/\partial Q_k|F\rangle$ with $\langle i|Q_k|f\rangle$. The normal mode Q_k is the same in both expressions. The latter $\langle i|Q_k|f\rangle$ requires normal harmonic oscillator selection rules (i.e., $f = i \pm 1$), and only those normal modes for which this term is nonzero will be observed. Note that this term implies that overtones will not normally be observed and that nontotally symmetric vibrations may be seen. However, an additional restriction on modes, which can be observed, is provided by the Herzberg−Teller coupling term h_{IF}, which must simultaneously be nonzero for the normal mode Q_k to be observed. This additional selection rule is crucial for understanding the details of SERS spectra. The other two terms in the numerator involve a product of the dipole transition moments $\mu^{\sigma}_{KI}\mu^{\rho}_{FK}$, which are the allowed molecular transition I−K and the (metal−molecule) charge-transfer transition F−K. The charge-transfer or molecular transition moment will depend on the molecular orientation with respect to the metal and therefore depends on the geometry of the molecule−metal complex. Since the maximum electric field due to the plasmon resonance is normal to the metal surface, we expect components of μ^{ρ}_{FK} and μ^{σ}_{KI} normal to the surface (i.e., $\rho, \sigma = Z$) to provide the major contribution to SERS. Weaker contributions from either σ or $\rho = X,Y$ will also be expected. Note that the combination of transition moments, Herzberg−Teller coupling,

and direction of the plasmon-induced electric field place restrictions on the nature of the spectrum and the symmetry of the normal modes expected to be observed. In the next section we examine the consequences of these restrictions for observed SERS spectra.

C. The Herzberg−Teller-Surface Selection Rules. As was shown in the previous section, the selection rules, which govern SERS intensity, are obtained by examination of the numerator in eq 12. In this section, we explore the implications of the product for metal−molecule charge transfer

$$\mu^{\sigma}_{\mathrm{KI}}\mu^{\rho}_{\mathrm{FK}}h_{\mathrm{IF}} = \langle \mathrm{I_e}|\mu^{\sigma}|\mathrm{K_e}\rangle\langle \mathrm{K_e}|\mu^{\rho}|\mathrm{F_e}\rangle\langle \mathrm{F_e}|\partial V_{\mathrm{eN}}/\partial \mathrm{Q_k}|\mathrm{I_e}\rangle \quad (16)$$

(or its counterpart for molecule-metal transfer obtained by interchanging I and K). For appreciable SERS intensity to appear, all three of these terms must simultaneously be nonzero. This imposes severe restrictions on the observed spectrum and provides a stringent test of the Herzberg−Teller theory. Note we have the additional surface selection rule imposed by the requirement that the plasmon resonance produce an electric field in large part perpendicular to the metal surface. Thus, we require that at least one of the transition moments μ_{FK} or μ_{KI} be polarized perpendicular to the surface in order for the normal mode to display much SERS intensity. This surface selection rule may be expressed in terms of a unit vector perpendicular to the surface $\hat{\mathbf{E}}^{\perp}$ such that $\mu_{\mathrm{FK}} = <\mathrm{F_e}|\mu\cdot\hat{\mathbf{E}}^{\perp}|\mathrm{K_e}>$ or expressed more simply: $<\mathrm{F_e}|\mu_{\mathrm{CT}}{}^{\perp}|\mathrm{K_e}>$. In order to account for this we require some knowledge of the geometry of the molecule−metal complex. The presence of the metal in the vicinity of a molecule will tend to lower the symmetry, relaxing some of the restrictions imposed. Of course, if the symmetry is lowered enough, all transitions will be allowed. If or when this is the case, we can have no valid test of the theory. However, it is found that in SERS, vibrational frequencies of the molecule are usually not shifted very much from those observed in the liquid or even gas phases. This implies that the molecule−metal interaction is not very strong, and the symmetry lowering effects may not be severe. In fact, we have found in the following examples that the only symmetry element we need to eliminate (by dropping the subscript *u* or *g*) is the inversion (where it exists) in order to satisfactorily explain the observed spectra.

We may also simplify the selection rules suggested by eq 16. Since each electronic state appears twice in the expression, together they belong to the totally symmetric irreducible representation. We need only consider symmetry species of the operators involved. Note also that $\Gamma(\mathrm{Q_k}) = \Gamma(\partial/\partial \mathrm{Q_k})$ and that, if the ground state $|\mathrm{I}\rangle$ is totally symmetric, then $\Gamma(\mu_{\mathrm{mol}}) = \Gamma_{\mathrm{K}}$. It can easily be seen that the simplest expression of the Herzberg−Teller-surface selection rules is

$$\Gamma(\mathrm{Q_k}) = \sum_{K} \Gamma(\mu_{\mathrm{CT}}^{\perp}) x \Gamma_{\mathrm{K}} \quad (17)$$

where $\Gamma(\mathrm{Q_k})$ is the irreducible representation to which the allowed SERS vibration belongs, $\Gamma(\mu_{\mathbf{CT}}{}^{\perp})$ is the irreducible representation to which the component of the charge-transfer dipole perpendicular to the surface belongs (in the combined molecule−metal system), and Γ_{K} is the irreducible representation of the molecular excited-state to which an optical transition is allowed ($\mathrm{I} \rightarrow \mathrm{K}$). Note that the sum runs over all the allowed (but presumably lower-lying) optical transitions. These latter transitions are those from which intensity is borrowed by the charge-transfer transition. Note that whenever $\Gamma(\mu_{\mathrm{CT}}{}^{\perp})$ is totally symmetric, we have the simplified selection rules

$$\Gamma(\mathrm{Q_k}) = \sum_{\mathrm{K}} \Gamma_{\mathrm{K}} \quad (18)$$

In the case of SERRS, this expression simplifies still further, by eliminating the sum over K, and $\Gamma(\mathrm{Q_k}) = \Gamma(\mu_{\mathbf{CT}}{}^{\perp}) x \Gamma_{\mathrm{k}}$ or for $\mu_{\mathrm{CT}}{}^{\perp}$ which is totally symmetric, $\Gamma(\mathrm{Q_k}) = \Gamma_{\mathrm{k}}$. The only nontotally symmetric state $|\mathrm{K}\rangle$ which contributes to SERRS is that for which the molecular resonance occurs.

We should at this point compare the Herzberg−Teller-surface selection rules with other selection rule schemes suggested to explain SERS. The most common are the surface selection rules discussed above. Note, the Herzberg−Teller-surface selection rules are quite similar to the surface selection rules (Section II.A), except that the charge-transfer or molecular resonance tends to pick out certain normal modes for additional resonant enhancement, and the relative contribution of each mode will be strongly wavelength or voltage dependent. This resonance effect can in principle be so large as to increase the nontotally symmetric intensities beyond those of the totally symmetric intensity at certain excitation wavelengths. We provide two good examples of this in the spectra of berberine (Figure 5) and *p*-aminothiophenol (Figure 6).

In developing the expression in eq 12 we used only the dipolar approximation for the induced electric dipole moment in the plasmon resonance effect. It has been suggested[44,45] that in addition to the electric dipole−electric dipole term a multipole expansion with a term in the electric dipole−electric quadrupole polarizability $\mathbf{A}_{\alpha\beta\gamma}$ should be important in the electromagnetic (EM) enhancement in SERS. This term

$$\frac{1}{3} A_{\alpha\beta\gamma} \frac{\partial E_{\beta}}{\partial \gamma} \quad (19)$$

is only significant for very large field gradients at the surface of the SERS metal active particle. This implies that the entire EM potential drop should be over a length on the order of the diameter of the molecule. Since the quadrupole polarizability tensor $\mathbf{A}_{\alpha\beta\gamma}$ transforms in the same way as the tensor in the nonlinear hyper-Raman effect, its application would introduce new Raman-active modes in SERS. Evidence for the appearance of some of these modes has been found in near-field optical microscopy experiments.[46] However, the spacer experiments of Murray[47] et al. showed that the Raman intensity is still observable several molecular diameters from the metal surface, indicating that the field does not drop significantly across the dimensions of a molecule. More recently, Van Duyne and coworkers[48] have compared the SERS modes with the surface-enhanced hyper-Raman scattering (SEHRS) modes for the same molecule under identical electrochemical conditions and find that the SERS and SEHRS spectra are distinctly different over a range of frequencies. They concluded that the symmetry of the molecule was not changed by adsorption and that "field gradient effects are negligible." This evidence shows for molecules on the surface of a single SERS-active metal particle that the EM effect is well modeled by the dipolar plasmon effect and that an analysis of the normal modes of a SERS spectrum need not include modes arising from the quadrupole polarizability tensor.

We now turn to the task of explaining the observed SERS spectra of several molecules using the Herzberg−Teller-surface selection rules. We choose mostly molecules with sufficiently high symmetry that will provide a real test of the theory. As pointed out elsewhere, anything can be explained with low enough symmetry, since almost everything is then allowed. We choose several azabenzenes, which form a weak Ag−N bond,

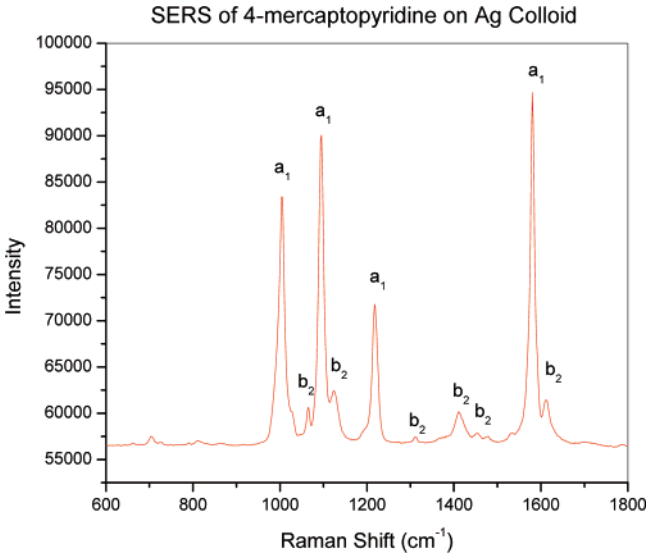

Figure 3. Surface-enhanced Raman spectrum of 4-mercapto-pyridine on Ag colloid. The symmetry species of the most enhanced modes (a_1 and b_2) are shown. All other modes are much weaker or not seen.

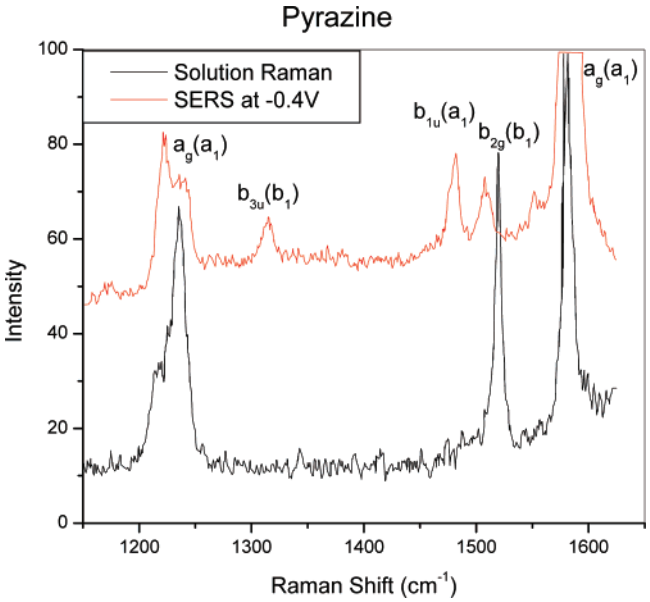

Figure 4. Surface-enhanced Raman spectrum of pyrazine on a Ag electrode, compared with that in solution. The symmetry of the modes is given in both D_{2h} and (C_{2v}) symmetry. See also Table 2. Note the enhancement of *u* modes, which are not seen in solution.

including pyridine, pyrazine, pyrimidine, pyridazine, and *s*-triazine. These all are of high symmetry and have the molecular plane perpendicular to the Ag surface. We further examine two molecules for which the molecular plane is parallel to the surface, namely, benzene and berberine. The former provides a good test of the theory because of its high symmetry, while the latter, even though it has lower symmetry, is of considerable interest due to the extremely high enhancement observed for the normally weak out-of-plane vibrations.

III. Applications to Individual Molecules: Test of the Herzberg−Teller-Surface Selection Rules

A. Pyridine. Since it was the first molecule in which SERS was discovered, pyridine (C_{2v}) is one of the most studied of all SERS-active molecules. We will not spend much time on this much-discussed molecule, except to illustrate how the Herzberg−Teller-surface selection rules can be applied. The SERS

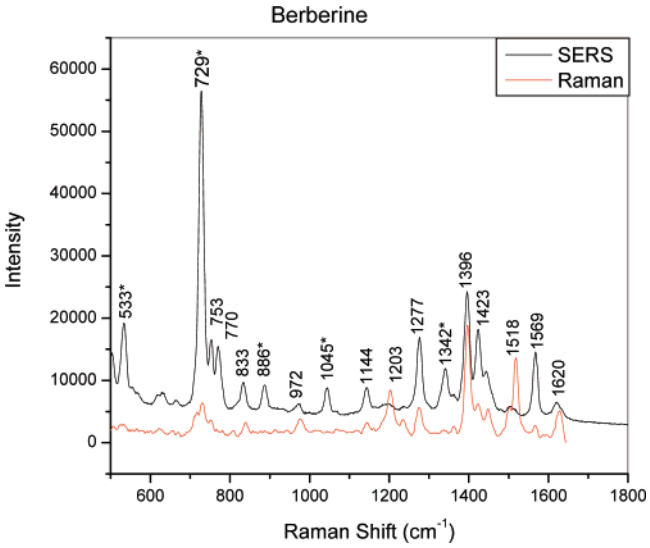

Figure 5. Surface-enhanced Raman spectrum of berberine on Ag colloid. Note that although there are almost no frequency shifts, the intensities of various lines are greatly enhanced or diminished in comparison to the normal Raman intensities by proximity to the surface. Lines marked with * are a″ modes, which are especially enhanced.

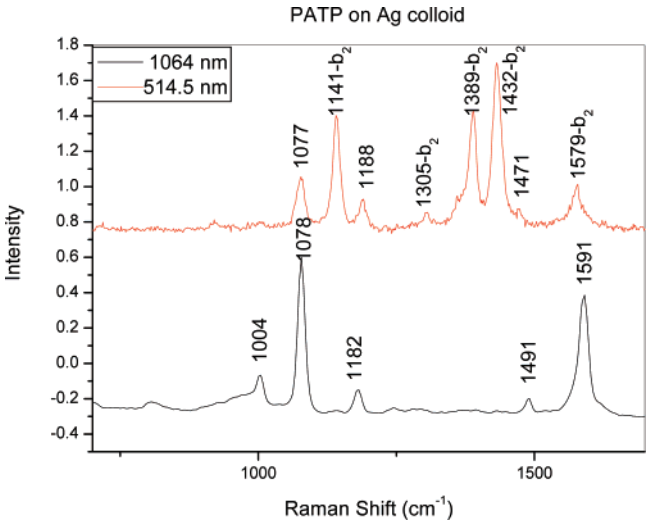

Figure 6. SERS of PATP on Ag colloid at 514.5 and 1064 nm. Lines of b_2 symmetry are marked, while all unmarked lines are of a_1 symmetry.

spectrum of pyridine (see Figure 2) is well-known to have modes, which are of a_1 and b_2 symmetry, as the most enhanced by proximity to the surface. Modes of b_1 and a_2 symmetry are barely seen, if at all. The molecule is attached to the surface through a weak Ag−N bond, using overlap of the nonbonding n electrons on the pyridine with the s electrons of the Ag surface atoms. This new bond is manifest through the appearance in the Raman spectrum of a new, rather broad line at around 240 cm^{-1}. The implication is that the molecule $C_2(z)$ axis (through the N) is perpendicular to the plane of the metal. This geometry results in no net lowering of symmetry due to the surface, and we may assume that the molecule−metal complex retains C_{2v} symmetry. In Table 1 we present the low-lying states of pyridine,[49] which are available for intensity borrowing. The lowest of these are the $n \rightarrow \pi^*$ ($^1B_1 \leftarrow {}^1A_1$, $f = 0.003$) transition at 34 770 cm^{-1}, the $\pi \rightarrow \pi^*$($^1B_2 \leftarrow {}^1A_1$, $f = 0.04$) transition at 38 350 cm^{-1}, and the $\pi \rightarrow \pi^*$ ($^1A_1 \leftarrow {}^1A_1$, $f = 0.10$) at 49 750 cm^{-1}. These restrict the possible symmetry species for the excited state K, which should be either B_1, B_2, or A_1. We now examine the possible symmetries of the charge-transfer state F.

TABLE 2: SERS of Pyrazine on a Ag Electrode at −0.4 V[a]

wavenumber	mode number	symmetry (D_{2h})	symmetry (C_{2v})
225	Ag−N		
440	16b	b_{2u}	b_2
636	6a	a_g	a_1
698	4	b_{3g}	b_2
743	10a	b_{1g}	a_2
800	11	b_{2u}	b_2
897	5	b_{3g}	b_2
1020	1	a_g	a_1
1237	9a	a_g	a_1
1317	14	b_{3u}	b_1
1488	19a	b_{1u}	a_1
1519	8b	b_{2g}	b_1
1597	8a	a_g	a_1
3074	2	a_g	a_1

[a] See ref 56.

Due to the surface plasmon restriction that the dipole operator for charge transfer be perpendicular to the metal surface and the geometry of the metal−molecule complex, for maximum enhancement, the dipole operator $\mu_{CT}^{\perp}$ in the expression $<F_e|\mu|K_e>$ must be of A_1 symmetry. This requires that the symmetry of F be B_1, B_2, or A_1. Using the selection rules (eq 17) we then see that Q_k must be of symmetry b_1, b_2, or a_1. However, the $n \rightarrow \pi^*$ ($^1B_1$) transition is quite weak ($f = 0.003$), and we expect b_1 modes to have only slight enhancement from intensity borrowing. Moreover, the $^1B_2$ and $^1A_1$ optical transitions are more than a factor of 10 stronger. Thus, we do not expect b_1 modes to be strongly enhanced, but predict strong enhancement of the b_2 and especially the a_1 modes. There are no optically allowed $^1A_2$ transitions, and we thus do not expect to see a_2 vibrations in SERS. This is exactly what is observed.

The same considerations may be applied to several related compounds, such as *p*-aminothiophenol (discussed in Section IV)[50−53] and 4-mercaptopyridine (see Figure 3).[54,55] In both cases the b_2 modes are strongly enhanced relative to the other modes. The molecules have the same orientation with respect to the surface as pyridine, and the lowest-lying available allowed optical transitions are of B_2 or A_1 symmetry ($\pi \rightarrow \pi^*$). As in pyridine, the b_1 and a_2 modes are predicted to be very weak, since no nearby intense optical transition of these symmetries is available for intensity borrowing.

B. Pyrazine, Pyrimidine, and Pyridazine. Pyrazine (1,4 diazabenzene), with inversion symmetry belongs to the point group D_{4h}. The SERS spectrum[56] of pyrazine on a Ag electrode at −0.4 V is shown in Figure 4, along with the solution spectrum. The measured wavenumbers along with their assignments and symmetry are listed in Table 2. It can be seen that on the surface, several bands of *u* symmetry appear, which are forbidden in the solution Raman spectrum. This, along with the appearance of the Ag−N line at 225 cm^{-1} indicate that, like pyridine, pyrazine is attached weakly to the surface with the molecular plane perpendicular to the surface. These observations lead to the conclusion that we can no longer maintain the inversion symmetry element, and the D_{2h} point group must be lowered to C_{2v}. Note that vibrations of several symmetry species are active in SERS, namely, a_g, b_{1g}, b_{1u}, b_{2g}, b_{2u}, b_{3g}, and b_{3u}. In Table 2, we also give the lowered species[57] corresponding to C_{2v}. Note that unlike pyridine, a_1, a_2, b_1, and b_2 vibrations appear. However, the a_1 and b_2 modes are most enhanced, while the b_1 and a_2 modes are somewhat less so. In Table 3, we present the allowed transitions observed in the UV spectrum of pyrazine.[49,58] In addition to the $n-\pi^*$ $^1B_{3u}$ ($^1B_1$, $f = 0.010$) at 3.83 eV, there are also two $\pi-\pi^*$ transitions at 4.69 eV $^1B_{2u}$ ($^1B_2$, $f = 0.010$) and 6.51 eV $^1B_{1u}$ ($^1A_1$, $f = 0.15$) and another $n-\pi^*$ ^1A_u ($^1A_2$, very weak) at 6.94 eV. We can now invoke the Herzberg−Teller-surface selection rules (eqs 17 or 18). The surface selection rule requires that the charge-transfer dipole moment operator ($\mu_{CT}^{\perp}$) be perpendicular to the surface, which in C_{2v} symmetry belongs to the A_1 irreducible representation. Thus, the charge-transfer state must be of symmetry B_1, B_2, A_1, and A_2, respectively corresponding to the four ultraviolet transitions. These in turn allow normal modes of b_1, b_2, a_1, and a_2 symmetry, just as observed. Note that the order of decreasing SERS enhancement ($a_1 > b_2 > b_1 > a_2$) is the same as the order of decreasing oscillator strength of the optical transitions. Similar conclusions were obtained by a somewhat different earlier analysis of Arenas et al.[59]

TABLE 3: UV Absorption Spectrum in Pyrazine[a]

transition	eV	symmetry D_{2h}	symmetry C_{2v}	intensity
$n \rightarrow \pi^*$	3.83	$^1B_{3u}$	$^1B_1$	$f = 0.010$
$\pi \rightarrow \pi^*$	4.69	$^1B_{2u}$	$^1B_2$	$f = 0.10$
$\pi \rightarrow \pi^*$	6.51	$^1B_{1u}$	$^1A_1$	$f = 0.15$
$n \rightarrow \pi^*$	6.94	^1A_u	$^1A_2$	vw

[a] See ref 49.

The surface-enhanced Raman spectrum of (C_{2v}) pyrimidine (1,3 diazine) was obtained by Centeno et al.[60] Briefly, all modes which are enhanced on the surface are either a_1 or b_2 symmetry. Once again, it is likely that the molecule is attached to the surface through a weak metal−nitrogen bond, and the molecular plane is perpendicular to the surface. Assuming no reduction in symmetry, the charge-transfer dipole polarization remains totally symmetric, and the simplified selection rules (eq 18) will hold. The electronic states of pyrimidine are given by Innes et al.[49] There are two $n \rightarrow \pi^*$ transitions at 3.85 and 6.34 eV, both of $^1B_1$ symmetry. These are extremely weak ($f = 0.0069$ and 0.005, respectively). Another $n \rightarrow \pi^*$ transition of $^1A_2$ symmetry is very weak and of questionable location. The only strongly allowed transitions are $\pi \rightarrow \pi^*$ transitions at 5.01 eV ($^1B_2$, $f = 0.052$) and 6.98 eV ($^1A_1$, $f = 0.16$). We thus expect to see the most enhancement for b_2 and a_1 modes, exactly as observed.

The surface-enhanced Raman spectrum of pyridazine (1,2 diazine) has been obtained by Takahashi et al..[61] Modes of symmetry a_1, b_1, and b_2 are observed, but no modes of a_2 symmetry are observed. Electronic transitions[49] are observed at 3.30, 4.90, and 6.20 eV corresponding to $^1B_1(n \rightarrow \pi^*, f = 0.0076)$, $^1A_1(\pi \rightarrow \pi^*, f = 0.020)$, and $^1B_2(\pi \rightarrow \pi^*, f = 0.10)$ symmetry, respectively. Once again, we assume that the molecular plane is perpendicular to the surface, and the charge-transfer dipole is therefore of A_1 symmetry. The first transition is fairly weak, but this is mitigated by the fact that it lies quite low in energy and might possibly be able to contribute intensity to b_1 vibrational modes. The other two transitions are stronger and easily explain the enhancement of the a_1 and b_2 vibrations. Note that there is no $^1A_2$ transition in the near UV region, so we might not expect a_2 modes to be present in the enhanced spectrum, and they are not.

C. *s*-Triazine. The SERS spectrum of (D_{3h}) *s*-triazine ($C_3H_3N_3$) was obtained by Moskovits et al.[62] and is presented in Table 4. Note however that the assignments given in the article were based on analogy with pyridine. A more recent work by Boese and Martin,[63] in which anharmonic force fields were combined with DFT calculations, gives a much better fit to the spectrum, with a few different assignments. We adopt their assignments and mode numbering here. Specifically, the modes at 344 and 1042 cm^{-1} were originally designated $\nu_{16}(e'')$ and

TABLE 4: SERS of *s*-Triazine[a]

mode no.	symmetry	SERS	intensity
14	a_2''	344	s
	e′	682	
	e′	693	
7	a_2''	727	m
6	a_2''	944	vw
3	a_1'	999	s
13	a_2''	1041	vw
2	a_1'	1125	s
11	e′	1164	m
	a_2'	1299	vw
10	e′	1407	w
10	e′	1410	m
9	e′	1555	s
9	e′	1575	
1	a_1'	3040	w

[a] See ref 62.

TABLE 5: Electronic States of *s*-Triazine[a]

state	symmetry	T_0 (cm^{-1})	type	intensity
X	$^1A_1$	0		
A	$^1A_2''$	31 574	$n \rightarrow \pi^*$	$f = 0.021$
B	$^1A_1''$, $^1E''$	32 500	$n \rightarrow \pi^*$	weak
C	$^1A_2'$	44 000	$\pi \rightarrow \pi^*$	$f = 0.002$
D	$^1A_2''$ or E′	55 782	R	strong

[a] Only the transitions to $^1A_2''$ and $^1E'$ are allowed, and all other transitions are either weak or diffuse. See ref 49.

ν_{10} (e″), but they are both of a_2'' symmetry in the more recent calculation. Two lines observed by Moskovits et al. (682 and 1299 cm^{-1}) are not assigned by Boese and Martin, but we have kept them in the table. Note that with the new assignments, only vibrations of symmetry a_1', a_2'', and e′ are strongly enhanced in the SERS spectrum. The line observed at 1299 cm^{-1} designated as a_2' is very weak.

The low-lying states of *s*-triazine are given in Table 5.[57,49] Note that although there are at least four transitions observed, only two at 31 574 cm^{-1} ($^1A_2''$) and 55 782 cm^{-1} ($^1A_2''$ or $^1E'$) are intense. The other transitions are weak and unlikely to contribute much intensity through intensity borrowing. We may now apply the Herzberg−Teller-surface selection rules. We assume that, like the other azabenzenes, *s*-triazine is attached to the surface through a weak Ag−N bond and that the molecular plane is perpendicular to the metal surface. In the molecule−metal system, the charge-transfer moment ($\mu_{CT}^{\perp}$) once again must be totally symmetric, leaving the simplified selection rules (eq 18). We then predict that both a_2'' and e′ vibrations will be enhanced by SERS. This is just what is observed, except for the a_1', which in any case are allowed by the A_k term (eq 13).

D. Benzene. The surface-enhanced Raman spectrum of benzene was obtained by Moskovits and co-workers[64,62] and is listed in Table 6. It is presumed to lie flat on the surface, and several Raman forbidden (IR-allowed) bands are observed in SERS, indicating a lowering of symmetry. The vibrational shifts are small, so that only a weak bond to the surface is indicated by the spectrum. This suggests we need only lower the symmetry to D_6, removing the center of symmetry in a direction perpendicular to the molecular plane. The most strongly surface-enhanced bands are $\nu_1(a_1)$, $\nu_{11}(a_2)$, $\nu_{16}(e_2)$, $\nu_{10}(e_1)$, and $\nu_8(e_2)$. $\nu_{14}(b_2)$ and $\nu_{15}(b_2)$ are weak, and no b_1 vibrations are observed.

The optical spectrum of benzene[57,65,66] is dominated by one forbidden transition to $^1B_{2u}$ ($^1B_2$) at 4.90 eV, ($f = 0.0014$), several more intense transitions $^1B_{1u}$ ($^1B_1$) at 6.20 eV, ($f = 0.094$), $^1E_{2g}$ ($^1E_2$) at 6.2 eV ($f = 0.094$), and $^1E_{1u}$ ($^1E_1$) at 6.90 eV ($f = 0.44$). Since the charge-transfer dipole moment perpendicular to the surface is also perpendicular to the molecule, $\Gamma(\mu_{CT}^{\perp}) = A_2$ (in D_6). Using the Herzberg−Teller-surface selection rules (eq 17), we therefore expect the strongest modes to be of e_1 (A_2xE_1) and e_2 (A_2xE_2) symmetry. We also predict weaker vibrations of b_2 (A_2xB_1) symmetry and still weaker vibrations of b_1 (A_2xB_2) symmetry. The observed b_2 modes are quite weak. The lack of observed b_1 modes results from the forbidden character of the $^1B_{1u}$ (B_2) UV transition. Thus, the Herzberg−Teller-surface selection rules match the observations. (Note that in any case, a_1 vibrations are active through the A terms, eqs 11 or 13).

TABLE 6: SERS of Benzene on a Ag Surface[a]

mode no.	SERS	intensity	D_{6h}	D_6
1	982	vs	a_{1g}	a_1
2	3060	w	a_{1g}	a_1
6	606	w	e_{2g}	e_2
8	1587	m	e_{2g}	e_2
9	1174	w	e_{2g}	e_2
10	864	m	e_{1g}	e_1
11	697	m	a_{2u}	a_2
14	1311	w	b_{2u}	b_2
15	1149	w	b_{2u}	b_2
16	397	m	e_{2u}	e_2
17	970	vw	e_{2u}	e_2
18	1032	vw	e_{1u}	e_1
19	1473	w	e_{1u}	e_1

[a] See ref 64.

E. Berberine. Berberine is a yellow-colored alkaloid dye used widely throughout the world for paper and textiles. It is an almost planar, partially conjugated molecule with five rings and has a positively charged N atom in the plane. The only symmetry element therefore will be reflection in the molecular plane, and therefore we may take the C_s point group to approximately represent the molecule. Figure 5 shows the normal Raman and FT SERS spectra of berberine[67]on Ag colloid excited at 785 nm. As is common in SERS, it can be seen that the frequencies are nearly identical to those of the normal Raman, while the relative intensities are wildly different. Note especially the lines at 533 (ν_{29}), 729 (ν_{40}), 886 (ν_{56}), 1045 (ν_{57}), and 1342 (ν_{82}) cm^{-1}. Several of these are not seen in the normal Raman spectrum, and all are strongly enhanced near the surface. In fact, the 729 cm^{-1} line is by far the most intense in the SERS spectrum. They all represent out-of-plane motions, and this, combined with the relative unavailability of nonbonding electrons (say from the nitrogen), indicates that the molecule lies flat on the surface, bonding weakly through the π-system of electrons. The yellow color indicates that there is a nearby allowed $\pi \rightarrow \pi^*$ ($A' \rightarrow A'$) transition available for intensity borrowing. This has been observed[68] at 421 nm, with an oscillator strength $f = 0.30$, while a more intense $\pi \rightarrow \pi^*$ ($A' \rightarrow A'$) transition has been observed in the ultraviolet at 342 nm ($f = 0.98$). Each is of sufficient intensity to provide ample intensity borrowing. The charge-transfer transition moment is both perpendicular to the metal and the molecular plane, so that $\Gamma(\mu_{CT}^{\perp}) = A''$, while the molecular transition moment $\Gamma_{p\rightarrow\pi^*} = A'$. Note that in this case the charge-transfer transition moment is not totally symmetric, and we must use the selection rules expression (eq 17). Thus, the vibrations which will be most enhanced will be out-of-plane a″ ($A'xA''$) vibrations, as observed. Although these conclusions could also have been arrived at without resort to symmetry arguments, the magnitude of the enhancement of out-of-plane modes in this case provides a good example of the effects of Herzberg−Teller coupling on SERS. It is also an example where the charge-transfer transition

moment is not totally symmetric in the molecule−metal system and of the coincidence of all three types of resonance contributions to SERS. In this case, the SERRS selection rule $\Gamma(Q_k) = \Gamma(\mu_{CT}^{\perp})x\Gamma_k$ applies. The nontotally symmetric a″ vibrations overwhelmingly dominate the spectrum, and the totally symmetric a′ modes, which in any case are always allowed by an A term, are comparatively weak.

IV. A Quantitative Measure of the Degree of Charge Transfer

A. Definition. We can obtain a quantitative measure of the relative charge-transfer contribution to the SERS intensity by defining $p_{CT}(k)$, the degree of charge transfer for each mode as

$$p_{CT}(k) = \frac{I^k(\mathrm{CT}) - I^k(\mathrm{SPR})}{I^k(\mathrm{CT}) + I^0(\mathrm{SPR})} \qquad (20)$$

where k is an index used to identify individual molecular lines in the Raman spectrum. We need the intensity of two reference lines obtained in a spectral region in which there is no charge-transfer contribution. One of these is I^k(SPR), the intensity of the line (k) in question taken where only the SPR contributes to the SERS intensity. This is ideally obtained in an electrochemical measurement at the same excitation wavelength (varying the applied potential) as that of the observed charge-transfer enhanced line. The other reference is a chosen totally symmetric line, also measured with only contributions from SPR. This is denoted I^0(SPR). I^k(CT) is the measured intensity of the line (k) in the region of the spectrum in which the charge-transfer resonance makes an additional contribution to the SERS intensity. Note that for a totally symmetric line $I^k(\mathrm{SPR}) = I^0(\mathrm{SPR})$, while for a nontotally symmetric line, I^k(SPR) will normally be small or zero. It can be seen from eq 20 that when p_{CT} is zero, there are no charge-transfer contributions, while as $p_{CT} \rightarrow 1$, the charge-transfer contributions will tend to dominate the spectrum. For $p_{CT} = {}^1/_2$, the charge-transfer and surface plasmon contributions are about equal.

Note also that we now have a quantitative way of separating the A-term contributions from the B- or C-term contributions. For totally symmetric modes p_{CT} gives the A-term contribution (unless there is additional contribution from intensity borrowing from a nearby totally symmetric optical transition via the B or C term). For nontotally symmetric modes, p_{CT} measures the B- or C-term contributions.

Although this approach is of some quantitative use, we should point out that it only applies to the contribution of a single mode to the overall enhancement. Each mode will display a different degree of charge transfer. This is due to the fact that the intensity of each nontotally symmetric mode is also proportional to the square of the Herzberg−Teller coupling constant (h_{IF} or h_{KF}), which has not been accounted for in this definition.

B. Charge-Transfer Contributions to the SERS in *p*-Amiothiophenol (PATP). The molecule PATP presents an excellent chance to examine quantitatively the relative contributions of surface plasmon resonance (SPR) and charge-transfer (CT) resonance terms to the overall enhancement. The experimental investigation by Osawa et al.[53] provides a rather complete picture of the electrochemical potential dependence as well as wavelength dependence, enabling detailed and quantitative analysis of the relative contributions, both near and far from the charge-transfer resonance. In Figure 6, we show the SERS spectrum of PATP at two considerably different excitation wavelengths (514.5 and 1064 nm). The spectrum at 514.5 nm is in the region of a metal-to-molecule charge-transfer transition,

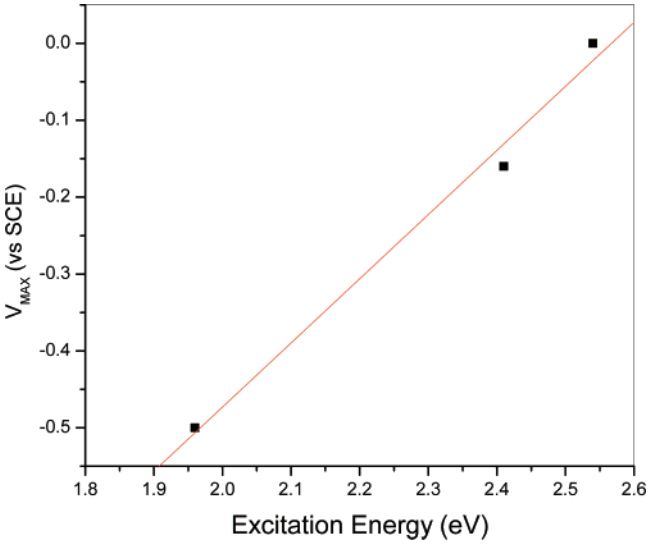

Figure 7. Potential maximum of the SERS of PATP signal as a function of excitation energy.

TABLE 7: Potential Dependence of Relative Intensities of the Lines of PATP at 1077 (a_1) and 1142 (b_2) cm^{-1} as a Function of Applied Potential, at Two Different Wavelengths (488 and 632 nm)

V (vs SCE)	I (1077 cm^{-1})	I (1142 cm^{-1})	p_{CT} (A term)	p_{CT} (C term)
		488 nm (2.54 eV)		
−0.20	1.4	1.8	0.22	0.67
−0.25	1.6	1.5	0.28	0.63
−0.30	1.2	0.7	0.14	0.44
−0.35	1.0	0.4	0.05	0.31
−0.40	0.9	0.2	0	0.18
−0.45	0.9	0.1	0	0.10
		632 nm (1.96 eV)		
−0.50	2.4	3.0	0.45	0.77
−0.60	2.1	2.9	0.40	0.76
−0.70	1.9	2.0	0.36	0.69
−0.75	1.4	1.0	0.22	0.52
−0.80	1.0	0.2	0.05	0.18

while that at 1064 nm is far from any molecular or charge-transfer resonance. Presumably, the enhanced 1064 nm spectrum involves only high-order surface plasmons in the nanoparticles. The spectrum at 514.5 nm shows several additional lines that are not observed at 1064 nm, and these dominate the spectrum. They are all of b_2 symmetry. All the lines observed at 1064 nm are totally symmetric (a_1) vibrations. Osawa et al. show that the appearance of strong lines of b_2 symmetry are due to intensity borrowing from an intense $\pi \rightarrow \pi^*$ molecular transition ($^1A_1 \rightarrow {}^1B_2$) at 300 nm.

Osawa et al. obtained potential dependent spectra at several different wavelengths (632, 514.5, and 488.0 nm). In Figure 7, we show a graph of the potential maxima (V_{MAX}) as a function of excitation energy. The positive slope of the curve and the fact that it is close to unity is taken as evidence of the metal → molecule charge-transfer nature of the spectral intensities. Their spectra show voltage dependent variations of both the totally symmetric (a_1) lines as well as of the nontotally symmetric (b_2) lines, and we can use these results to determine the degree of charge-transfer contributions from both the A term and C term (metal-to-molecule) in the SERS spectrum. In Table 7 we present the measured relative intensities of two selected lines: the 1077 cm^{-1} (a_1) vibration and the 1142 cm^{-1} (b_2) vibration as a function of applied potential (V vs SCE). These are chosen because they are relatively intense, well separated from other nearby lines and are close to each other. In order to obtain a

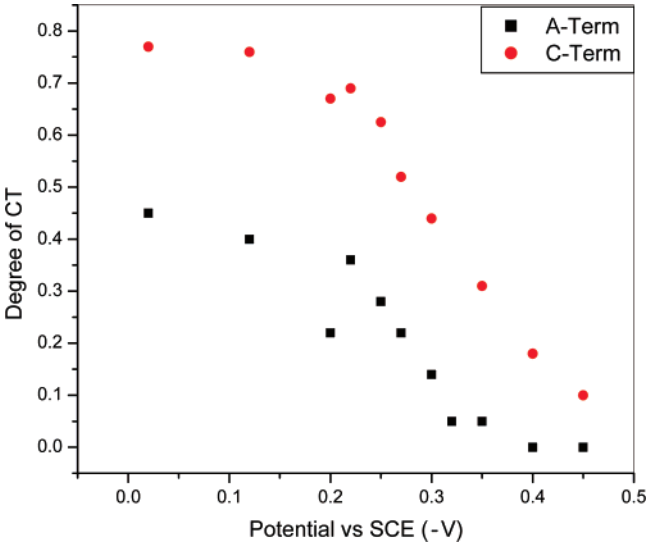

Figure 8. Degree of charge transfer for PATP as a function of applied potential for the 1077 cm^{-1} (a_1) line (squares) and the 1141 cm^{-1} (b_2) line (dots). The former represent the A-term contributions and the latter represent the C-term (Herzberg−Teller) contributions to the SERS intensity.

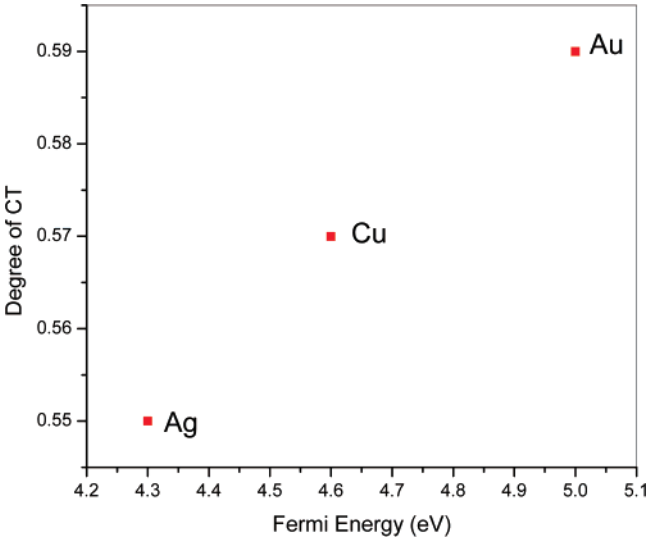

Figure 9. Degree of charge transfer as a function of Fermi Energy for PATP on roughened coinage metal foils excited at 632 nm.

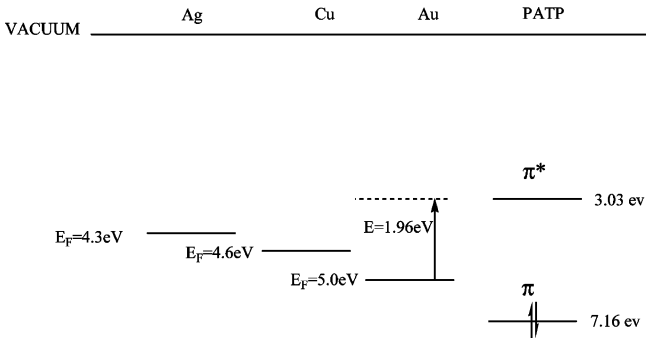

Figure 10. Fermi levels of Ag, Cu, and Au and molecular orbitals of PATP. Note that the 632 nm line (1.96 eV) is in resonance with the charge-transfer transition from the Fermi level of Au to the π^* level of PATP.

quantitative measure of the relative contribution of the charge-transfer transition to the overall SERS intensity, we take as a reference the intensity of the a_1 line in a region of potential in which there is no charge transfer at each wavelength. For excitation at 488 nm, we choose the spectrum at −0.45 V, and for excitation at 632 nm we choose the spectrum at −0.80 V. The reference intensities of the totally symmetric line are I^0(SPR) 0.9 and 1.0, respectively. We also need a reference intensity of the observed line (labeled k) in the region in which charge transfer is absent. I^k(SPR) is zero for $k = b_2$ and equal to I^0(SPR) for $k = a_1$.

For the a_1 line of PATP, we obtain the degree of charge transfer from the A term, while for the b_2 line we obtain that for the C term. These are calculated in the last two columns of Table 7 and displayed graphically as a function of applied potential in Figure 8. In determining this graph we corrected for the wavelength dependence of the potential by adding 0.50 V to potentials associated with the 632 nm line. This gives them a common origin (see Figure 7). Note that as the potential becomes less negative the degree of charge transfer increases, while the C-term contribution is about twice that of the A-term contribution. At the maximum, near the potential of 0.0 V, the C-term degree of charge transfer is nearly 0.8.

We may now use this quantitative measure of charge transfer to examine the effect of other properties on the SERS intensity. For example Shin et al.[69] have obtained the SERS spectra of PATP at 623 nm (1.96 eV) on roughened foils of Cu, Ag, and Au. The Fermi energy for these foils varies as Cu (4.6 eV), Au (5.0 eV), and Ag (4.3 eV). In Figure 9 we plot the degree of charge transfer of the 1142 cm^{-1} line as a function of Fermi energy. Note that the degree of charge transfer tends to increase with increasing Fermi energy. This can be explained by reference to Figure 10, where we plot the Fermi levels of the metals from the vacuum, along with the π and π^* levels of PATP. The ionization potential of PATP is 7.16 eV,[70] which locates the filled π orbital. The lowest unfilled π^* orbital (LUMO) should correspond to the 300 nm transition, putting it at 3.03 eV. Note that the laser excitation at 632 nm (1.96 eV) is in resonance with the charge-transfer transition from the Au Fermi level to the π^* molecular level, and the increasing degree of charge-transfer shown in Figure 9 represents the increasing approach to this resonance.

V. Conclusions

We have presented a unified expression for surface-enhanced Raman spectroscopy (SERS). The expression contains a product of three resonance denominators, representing the surface plasmon resonance, the molecule−metal charge-transfer resonance at the Fermi energy, and an allowed molecular resonance. We examined first the sources of intensity for wavelengths at which only surface plasmon resonances are active. This involves a sum over many terms, but these may be sorted by symmetry, and the leading terms in each of the sums derive from the lowest-lying transitions of the molecule−metal system. Using these expressions, we reexamine the surface selection rules and discuss the most important contributions to the SERS signal in that region. We then examined the implications for the spectrum of overlap of the charge transfer or molecular transitions with the plasmon resonance. We showed that vibrations of certain symmetries will be selectively enhanced in this region. We also then explored the Herzberg−Teller-surface selection rules. We showed that the three resonances may not be treated as independent since they are linked by a product of four matrix elements in the numerator. These linked matrix elements are responsible for the selection rules of SERS. One involves a harmonic oscillator in the observed normal mode, which gives normal harmonic oscillator selection rules, as opposed to the

usual resonance Franck−Condon selection rules. This is the same mode as that involved in the vibronic coupling (Herzberg−Teller) matrix element, so that only normal modes with the same symmetry as the Herzberg−Teller coupling operator are allowed. There is also the product of two transition dipole moments, resulting in a dependence of the SERS intensities on the oscillator strengths of the transitions involved. The charge-transfer transition moment is further linked to the surface plasmon resonance by the requirement that the transition dipole moment is polarized parallel to the direction of maximum amplitude of the field produced by the plasmon. In order to test the theory, we apply these selection rules to the spectra of several molecules of high symmetry including various azabenzenes, benzene, and berberine. In all these cases we are able to explain the observed spectrum using only the Herzberg−Teller-surface selection rules.

We then introduced a quantitative measure of the degree of charge transfer, which was used to examine the charge-transfer contributions to the SERS spectrum of PATP under various conditions. It is important for all quantitative determinations of the relative contributions to the SERS intensity that accurate spectra be obtained at various different excitation wavelengths, electrochemically at a variety of applied potentials, or utilizing a variety of particle sizes and shapes. Furthermore, good absorption spectra are needed to provide parameters of the various resonances as well as measures of the oscillator strengths. The only additional parameter needed to explain the SERS intensities is the magnitude of the vibronic (Herzberg−Teller) coupling constant (h_{SR}). This has been found to be difficult to measure experimentally. It has been shown to be related to the polaron coupling constant in solids (II),[36] but attempts to calculate it for molecule−metal systems have not been satisfactory. With the advent of time-dependent density functional theory, it is possible that accurate calculations of vibronic interactions may be successful.

In this Article, we have examined a way to approach SERS by careful examination of the various terms involved in the expression for the polarizability of the molecule−metal system. We have shown that in any region of the spectrum in which only a surface plasmon is active, the surface selections rules may be utilized. This predicts that the totally symmetric bands will tend to dominate the spectrum, but that, depending on the relative magnitudes of the normal and tangential fields, the nontotally symmetric contributions can be observed. In addition, despite the fact that charge transfer is not in resonance, these transitions, which come about by consideration of the combined molecule−metal system, cannot be ignored and may contribute significantly to the intensity of both totally and nontotally symmetric modes. It is important to recognize that when determining the enhancement factor, the polarizability tensor (eq 10) including the interaction of the molecule with the metal can add new terms to the expression not found in the corresponding expression in the absence of a surface (i.e., the normal Raman spectrum). When a charge-transfer or molecular resonance is also involved, additional intensity contributions from nontotally symmetric vibrations can be obtained, and under certain circumstances these can even come to dominate the spectrum. To fully determine the magnitude of the contributions from each effect, it is important that in addition to SERS spectra obtained at a variety of wavelengths, applied potentials, and nanoparticle sizes and distances, it is also necessary to obtain good values for other optical properties of the molecule−metal system, such as locations of the optical transitions, their oscillator strengths, and homogeneous linewidths. Only then can an accurate assessment be made as to the source of various contributions to the SERS intensities. If we excite in the region of a charge-transfer or molecular resonance, the enhancement of the nontotally symmetric bands relative to the totally symmetric bands will vary as we scan through the resonance. In the absence of charge-transfer contributions, the relative enhancement of both types of bands should be the same, regardless of the excitation wavelength or potential.

Acknowledgment. We would like to thank Richard Livingstone, Catherine Chenal, and Dr. Jie Zhang for assistance in preparing this Article. We are indebted to the National Institute of Justice (Department of Justice Award No. 2006-DN-BX-K034) and the City University Collaborative Incentive program (No. 80209). This work was also supported by the National Science Foundation under Cooperative Agreement No. RII-9353488, Grant No. CHE-0091362, CHE-0345987, and Grant No. ECS0217646 and by the City University of New York PSC-BHE Faculty Research Award Program. This research was also supported by the NIH/NIGMS/SCORE Grant No. GM08168 and a NCSA Grant No. CHE050065 for computer facilities.

References and Notes

(1) Fleischmann, M. P. J.; Hendra, A. J.; McQuillan, A. J. *Chem. Phys. Lett*. **1974**, *26*, 63.

(2) Van Duyne, R. P. *Chemical and Biochemical Applications of Lasers*; Moore, C. B., Ed.; Academic Press: New York, 1979; Vol. 4, Chapter 5.

(3) Furtak, T. E. *Advances in Laser Spectroscopy*; Garetz, B., Lombardi, J. R., Eds.; Wiley: Chichester, U.K., 1984; Vol. 2, p 175.

(4) Birke, R. L.; Lombardi, J. R. *Advances in Laser Spectroscopy*; Garetz, B., Lombardi, J. R., Eds.; Heyden: Philadelphia, PA, 1982; Vol. 1, p 143.

(5) Furtak, T. E.; Macomber, S. H. *Chem. Phys. Lett.* **1983**, *95*, 328.

(6) Billman, J.; Otto, A. *Solid State Commun.* **1982**, *44*, 105.

(7) Lombardi, J. R.; Birke, R. L.; Sanchez, L. A.; Bernard, I.; Sun, S. C. *Chem. Phys. Lett*. **1984**, *104*, 240.

(8) Burstein, E.; Chen, Y. J.; Lundquist, S.; Tosatti, E. *Solid State Commun.* **1979**, *21*, 567.

(9) Perrson, B. N. J. *Chem. Phys. Lett.* **1981**, *82*, 561.

(10) Gersten, J. I.; Birke, R. L.; Lombardi, J. R. *Phys. Rev. Lett*. **1979**, *43*, 147.

(11) Nie, S.; Emory, S. R. *Science*, **1997**, *275*, 1102.

(12) Kneipp, K.; Wang, Y.; Kneipp, H.; Perelman, L.; Itzkan, I.; Dasari, R. R.; Feld, M. S. *Phys. Rev. Lett*. **1997**, *78*, 1667.

(13) Xu, H.; Bjerneld, E.; Käll, M.; Börjesson, L. *Phys. Rev. Lett*. **1999**, *83*, 4357.

(14) Schatz, G. C., Young, M. A., Van Duyne, R. P. *Surface-Enhanced Raman Scattering-Physics and Applications*; Kneipp, K., Moskovits, M., Kneipp, H., Eds.; Topics in Applied Physics; Springer Berlin: Heidelberg, 2006; Vol. 103, pp 19−46.

(15) Michaels, A. M.; Jiang, J.; Brus L. E. *J. Phys. Chem. B* **2000**, *104*, 11965.

(16) Bosnick, K. A.; Jiang, J.; Brus, L. E. *J. Phys. Chem. B* **2002**, *106*, 8096.

(17) Bosnick, K. A.; Jiang, J.; Brus, L. E. *J. Phys. Chem. B.* **2002**, *106*, 11965.

(18) LeRu, E. C.; Blackie, E.; Meyer, M.; Etchegoin, P. G. *J. Phys. Chem. C* **2007**, *111*, 13794−13803.

(19) McFarland, A. D.; Young, M. A.; Dieringer, J. A.; Van Duyne, R. P. *J. Phys. Chem. B* **200**5, *109*, 11279−11285.

(20) Zheng, X.; Xu, W.; Corredor, C.; Xu, S.; An, J.; Zhao, B.; Lombardi, J. R. *J. Phys. Chem. C* **2007**, *111*, 14962−14967.

(21) Lee, S. J.; Guan, Z.; Xu, H.; Moskovits, M. *J. Phys. Chem. C* **200**7, *111*, 17985−17988.

(22) Xue, C.; Mirkin, C. A. *Angew. Chem., Int. Ed.* **2006**, *46*, 2036−2038.

(23) Chang, R. K.; Laube, B. L. In CRC *Critical Reviews in Solid State and Materials Science*; CRC Press, Inc.: Boca Raton, FL, 1984; Vol. 12, pp 1−73, .

(24) Van Duyne, R. P. In *Chemical and Biochemical Applications of Lasers*; Moore, C. B., Ed.; Academic Press: New York, 1979; Vol. 4, pp 101−185.

(25) Lombardi, J. R.; Birke, R. L. *Surface Enhanced Raman Scattering*. In *Spectro-electrochemistry: Theory and Practice*; Gale, R. J., Ed.; Plenum Press: New York, 1988.

(26) Corni, S.; Tomasi, J. *J. Chem. Phys.* **2002**, *114*, 3739.
(27) Rojas, R.; Claro, V. F. *J. Chem. Phys.* **1993**, *98*, 998−1006.
(28) Gersten, J. I.; Nitzan, A. In *Surface Enhanced Raman Scattering*; Chang, R. K., Furtak, T. E., Eds.; Plenum Press: New York, 1982.
(29) Gersten, J.; Nitzan, A. *Surf. Sci.* **1985**, *158*, 165.
(30) Xu, H.; Bjerneld, E. J.; Käll, M.; Börjesson, L. *Phys. Rev. Lett.* **1999**, *83*, 4357.
(31) Xu, H.; Aizpuruna, J.; Käll, M.; Apell, P. *Phys. Rev. E*: *Stat., Nonlinear, Soft Matter Phys.* **2000**, *62*, 4318.
(32) Kramers, H. A.; Heisenberg, W. *Z. Phys*. **1925**, *31*, 681.
(33) Dirac, P. A. M. *Proc. R. Soc. London, Ser. A.* **1927**, *114*, 710.
(34) Albrecht, A. C. *J. Chem. Phys*. **1961**, *34*, 1476.
(35) Lombardi, J. R.; Birke, R. L.; Lu, T.; Xu, J. *J. Chem. Phys*. **1986**, *84*, 4174.
(36) Lombardi, J. R.; Birke, R. L. *J. Chem. Phys* **2007**, *126*, 244709.
(37) Albrecht, A. C. *J. Chem. Phys.* **1960**, *33*, 156−169.
(38) Albrecht, A. C. *J. Chem. Phys.* **1960**, *33*, 169−178.
(39) Yamada, H.; Nagata, H.; Toba, K.; Nakao, Y. *Surf. Sci*. **1987**, *182*, 269−286.
(40) Moskovits, M. *J. Chem. Phys.* **1982**, *77*, 4408−4416.
(41) Hexter, R. M.; Albrecht, M. G. *Spectrochim. Acta, Part A* **1979**, *35*, 233. Nichols, H.; Hexter, R. M. *J. Chem. Phys*. **1981**, *74*, 3126.
(42) Richardson, N. V.; Sass, J. K. *Chem. Phys. Lett*. **1979**, *62*, 267.
(43) Moskovits, M. *J. Chem. Phys*. **1982**, *77*, 4408.
(44) Sass, J. K.; Neff, H.; Moskovits, M.; Holloway, S. *J. Chem. Phys.* **1981**, *85*, 621−623.
(45) Ayars, E. J.; Hallen, H. D.; Jahnke, C. L. *Phys. Rev. Lett.* **2000**, *85*, 4180.
(46) Ayars, E. J.; Jahncke, C. L.; Paesler, M. A.; Hallen, H. D. *The Sixth International Conference on Near-field Optics and Related Techniques*, 2000, University of Twente, The Netherlands.
(47) Murray, C. A.; Allara, D. L.; Rhinewine, M. *Phys. Rev. Lett.* **1981**, *46*, 57.
(48) Hulteen, J. C.; Young, M. A.; Van Duyne, R. P. *Langmuir* **2006**, *22*, 10354−10364.
(49) Innes, K. K.; Byrne, J. P.; Ross, I. G. *J. Mol. Spectroscr*. **1967**, *22*, 125−147.
(50) Hu, X.; Wang, T.; Wang, L.; Dong, S. *J. Phys. Chem. C* **2007**, *111*, 6962−6969.
(51) Zhou, Q.; Zhao, G.; Chao, Y.; Li, Y.; Wu, Y.; Zheng, J. *J. Phys. Chem. C* **2007**, *111*, 1951−1954.
(52) Cao, L.; Diao, P.; Tong, L.; Zhu, T.; Liu, Z. *Chem. Phys. Chem.* **2005**, *6*, 913−918.
(53) Osawa, M.; Matsuda, N.;Yoshii, K.; Uchida, I. *J. Phys. Chem*. **1994**, *98*, 12702−12707.
(54) Baldwin, J.; Schüler, N.; Butler, I. S.; Andrews, M. P. *Langmuir* **1996**, *12*, 6389−6398.
(55) Wang, Y.; Sun, Z.; Hu, H.; Jing, S.; Zhao, B.; Xu, W.; Zhao, C.; Lombardi, J. R. *J. Raman Spectrosc.* **2007**, *38*, 34−38.
(56) Erdheim, G. R.; Birke, R. L.; Lombardi, J. R. *Chem. Phys. Lett.* **1980**, *69*, 495−498.
(57) Herzberg, G. *Electronic Spectra of Polyatomic Molecules*; D. Van Nostrand Co.: New York, 1966.
(58) Weber, P.; Reimers, J. R. *J. Phys. Chem. A* **1999**, *103*, 9821−9829. Walker, I.; Palmer, M. H. *Chem. Phys.* **1991**, *153*, 169−187.
(59) Arenas, J. F.; Woolley, M. S.; Lopez Tocon, I.; Otero, J. C.; Marcos, J. I. *J. Chem. Phys*. **2000**, *112*, 7669.
(60) Centeno, S. P.; Lopez-Tocon, I.; J. Arenas, J. F.; Otero, J. C. *J. Phys. Chem. B* **2006**, *110*, 14916−14922.
(61) Takahashi, M.; Niwa, M.; Ito, M. *J. Phys. Chem*. **1987**, *91*, 11−14.
(62) Moskovits, M.; DiLella, D. P.; Maynard, K. J. *Langmuir* **1988**, *4*, 67−76.
(63) Boese, A. D.; Martin, J. M. L. *J. Phys. Chem. A* **2004**, *108*, 3085−3096.
(64) Moskovits, M.; DiLella, D. P. *J. Chem. Phys.* **1980**, *73*, 6068−6075.
(65) Albrecht, A. C. *J. Chem. Phys.* **1960**, *33*, 169−178.
(66) Zeigler, L. D.; Hudson, B. *J. Chem. Phys.* **1981**, *74*, 982−992.
(67) Leona, M.; Lombardi, J. R. *J. Raman Spectrosc.* **2007**, *38*, 853−858.
(68) Strekal, N. D.; Motevich I. G.; Nowicky, J. W.; Maskevich, S. A. *J. Appl. Spectrosc.* **2007**, *74*, 3137.
(69) Shin, K. S.; Lee, H. S.; Joo, S. W.; Kim, K. *J. Phys. Chem. C* **2007**, *111*, 15223−15227.
(70) Larsen, A. G.; Holm, A.; Roberson, M.; Daasbjerg, K. *J. Am. Chem. Soc.* **2001**, *123*, 1723−1729.